Contrib Mineral Petrol (2009) 158:17–36
DOI 10.1007/s00410-008-0368-z

ORIGINAL PAPER

Interactions between dioritic and granodioritic magmas in mingling zones: plagioclase record of mixing, mingling and subsolidus interactions in the Gęsiniec Intrusion, NE Bohemian Massif, SW Poland

Anna Pietranik · Jürgen Koepke

Received: 11 July 2007 / Accepted: 12 December 2008 / Published online: 10 January 2009

Abstract Dioritic and granodioritic rocks coexist in the Gęsiniec Intrusion in SW Poland showing typical relationships in many mafic–felsic mingling zones worldwide, such as dioritic syn-putonic dykes and microgranular enclaves within granodioritic host. Plagioclase zonation from granodioritic rocks suggests late stage mixing probably with dioritic magma, whereas no magma mixing is recorded in plagioclase from dioritic rocks. The diorites seem to show effects of interaction with evolved, leucocratic melts derived from granodiorite, not with the granodioritic melt itself. We conclude that the diorites' compositions were modified after their emplacement within the granodioritic host, when the diorites were essentially solidified and injection of evolved melt from granodiorite did not involve marked modification of plagioclase composition. Compositional zoning patterns of plagioclase in diorites can be modeled by closed system fractional crystallization interrupted by resorption induced probably by decompression. Granodioritic plagioclase seems to be affected by the same resorption event. Plagioclase that crystallized in dioritic magma before the resorption does not record interaction between dioritic and granodioritic magmas, suggesting that both magmas evolved separately.

Keywords Magma mingling · Magma mixing · Subsolidus interactions · Diorite · Granodiorite · Plagioclase · Sr · Bohemian Massif

Communicated by B. Collins.

Electronic supplementary material The online version of this article (doi:10.1007/s00410-008-0368-z) contains supplementary material, which is available to authorized users.

A. Pietranik (✉)
Institute of Geological Sciences, University of Wrocław,
pl. Borna 9, 50-205 Wrocław, Poland
e-mail: apietranik@gmail.com; anna.pietranik@ing.uni.wroc.pl

J. Koepke
Institute of Mineralogy, University of Hannover,
Callinstraße 3, 30167 Hannover, Germany

Introduction

Production of continental crust involves interaction between mafic, mantle-derived and felsic, crustally derived magmas that may occur at different crustal levels and lead to production of a variety of hybrid magmas (Annen et al. 2006; Bonin 2004; Kemp et al. 2007).Understanding mechanisms of mafic and felsic magma interaction is therefore essential to understand the processes of continental crust formation. Direct evidence of the interaction between mafic and felsic magmas can be seen in numerous outcrops with spectacular magmatic structures that include mafic synplutonic dykes, mafic–felsic layered intrusions and mafic microgranular enclaves within the more felsic host (e.g., Didier and Barbarin 1991). The field evidence, such as chilled and crenulate margins of the enclaves, hybrid zones at the mafic–felsic contacts, back-veining, and similar xenocrysts in both magmas, suggests thermal disequilibrium and mingling between mafic and felsic magmas after injection of the hotter mafic magma into the colder felsic one (Altherr et al. 1999; Dorais et al. 1990; Elburg 1996; Kumar and Rino 2006; Tepper and Kuehner 2004; Waight et al. 2000; Waight et al. 2001). Most of the chemical variation observed in the more mafic magmas is explained by mixing or diffusional equilibration between mafic and felsic magmas that occurred before mafic magma was injected and distributed as mafic enclaves in the felsic

host (Elburg 1996; Kumar and Rino 2006; Tepper and Kuehner 2004). Usually, the dioritic, moznonitic to tonalitic enclaves form by mingling and mixing during contemporaneous ascent or emplacement of mafic and felsic magmas (Barbarin 2005; Collins et al. 2000). In this paper we seek to test this hypothesis by analyzing plagioclase grains from a typical mafic–felsic mingling zone. Plagioclase appears to be the only mineral that does not equilibrate during interactions between mafic and felsic magmas (Tepper and Kuehner 2004) and may preserve information about mixing–mingling processes that affected mineral and whole-rock composition of co-mingled mafic and felsic rocks. The data are for plagioclase (anorthite and Sr contents) and whole rock compositions from variably hybridized dioritic to granodioritic rocks from the Variscan Gęsiniec Intrusion (NE Bohemian Massif, Poland).

Geological setting and field relationships

The samples analyzed in this study are from the Variscan Gęsiniec Intrusion in the northern part of the Strzelin Massif in SW Poland, the NE Bohemian Massif. The Strzelin Massif (SM) outcrops as a N–S elongated block 35 km south of Wrocław between 50°38′–50°46′N and 17°00′–17°10′E. It is composed of metamorphic basement of Precambrian to Devonian age intruded by Variscan granodiorites, tonalites, quartz diorites, biotite granites, and two-mica granites (Oberc-Dziedzic et al. 1996, 2003). The Pb-evaporation zircon age of biotite granite is 301 ± 7 Ma (Turniak et al. 2006), whereas a whole rock Rb–Sr isochron yielded an age of 347 ± 12 Ma (Oberc-Dziedzic et al. 1996). Quartz diorites from the Gęsiniec Intrusion yielded Rb–Sr biotite + whole rock + plagioclase ages of 295 ± 0.6 Ma and 307 ± 4.8 Ma (Pietranik and Waight 2008) and zircon Pb-evaporation ages from 280.9 ± 9 to 302.8 ± 8.6 Ma (Turniak et al. 2006).

The tonalite-diorite rocks in SM occur as separate intrusions, mostly dykes (Oberc-Dziedzic 2002), and as fine-grained enclaves within biotite granite and granodiorite (Lorenc 1984). Dykes are several metres to several tens of metres thick and were described mainly from borehole material (Oberc-Dziedzic 2002). The exception is the Gęsiniec Intrusion which is several-hundred-metre thick and outcrops in an active quarry (Fig. 1).

The Gęsiniec Intrusion is dominated by tonalite and quartz diorite and contains three main magma pulses: tonalitic-dioritic, granodioritic-tonalitic and granitic (Oberc-Dziedzic 1999, Pietranik and Waight 2008). Dioritic to granodioritic rocks penetrated each other and are crosscut by leucocratic veins. Granitic veins and bodies are the youngest and they crosscut the diorites, tonalites, diorites, and leucocratic veins. The inner parts of the intrusion are composed of medium to coarse-grained diorite to tonalite (Pietranik and Waight 2008), whereas the outer parts of the intrusion are dominated by fine-grained diorite to quartz diorite and granodiorite showing various structures typical for mafic–felsic magma mingling (Figs. 1, 2).

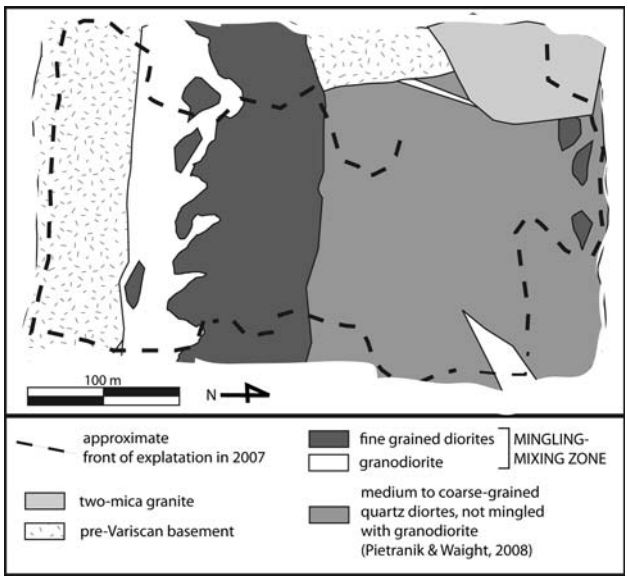

Fig. 1 Simplified plan of the Gęsiniec quarry showing distribution of different lithologies

Sampling and analytical methods

Ten samples were chosen for this study (Fig. 2) from the mingling-mixing zone (Fig. 1). They include diorite and quartz diorite (D10, D30, D27) from the massive dioritic bodies, rocks from the complex mingling zone (two quartz dioritic enclaves E48, E32 and one granodiorite GD31 surrounding the enclave E32), granodiorite (samples of veins crosscutting quartz diorite and tonalite GD15, GD16, and one from a larger body of granodiorite showing a complex crenulated contact with diorite GD55), and one sample of leucocratic vein (LV42).

Whole rock geochemical analyses for twelve samples were done in the ACME Analytical Laboratory (Canada/Vancouver). Major elements were analyzed by ICP-ES and trace elements were analyzed by ICP-MS following fusion of samples in $LiBO_2/Li_2B_4O_7$. The analytical reproducibility (2SD), as estimated from duplicate analysis of sample E31, ranges from 2 (LREE) to 20% (U) at 95% confidence limits. Analytical accuracy (2SD), as estimated from measurements of standard SO18/CSC is from 3 (La) to 22% (Rb) at 95% confidence limits.

Three samples (D15, D48, D27) were analyzed for whole rock Sr and Nd isotopes following techniques described in Pietranik and Waight (2008).

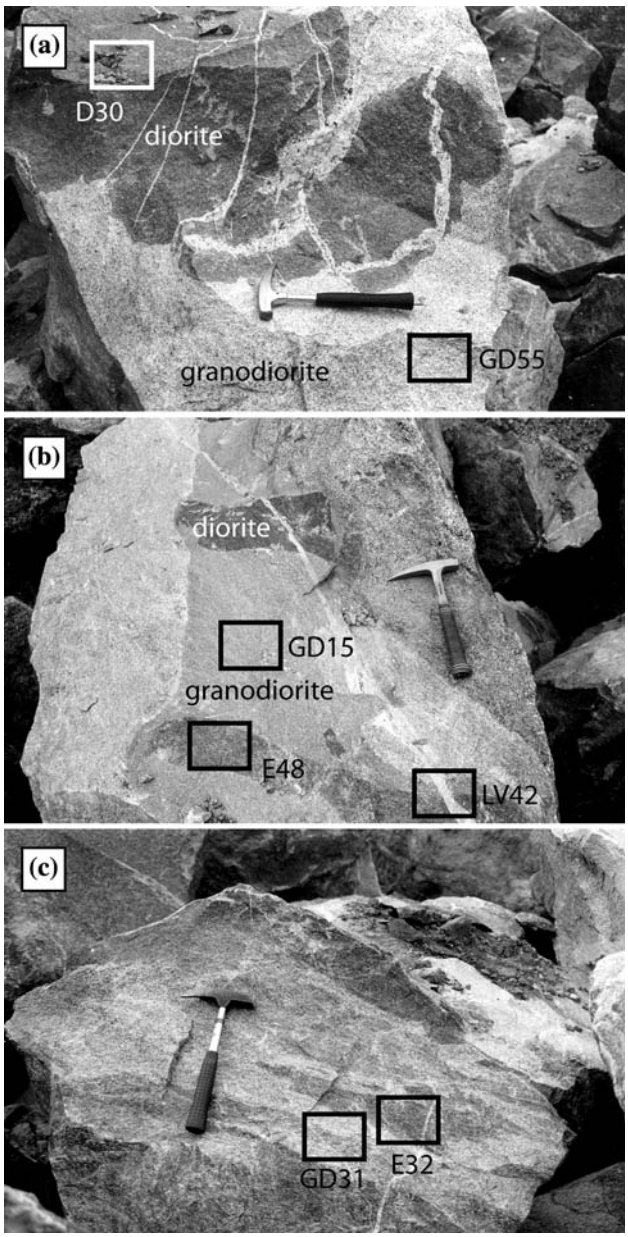

Fig. 2 Field relationships between granodiorite and diorite in the Gęsiniec Intrusion with approximate places of sampling (*rectangles*). **a** Contact between granodiorite and disrupted diorite dyke, note back-veining of granodiorite into diorite, **b** complex mingling zone, elongated quartz dioritic enclaves within granodioritic host, all rocks are crosscut by a fine-grained leucocratic vein, **c** granodioritic vein containing dioritic enclaves

The mineral compositions were analyzed on a CAMECA SX100 microprobe at the Institute of Mineralogy, University of Hannover. Analytical conditions were 20 kV acceleration voltage, 40nA sample current, beam defocused to 2 μm, 10 s counting time for peak and background for major elements and 180 s/90 s counting time for peak and background for Sr. The detection limit of Sr was ~150 ppm.

Petrography

A summary of the petrography and the modal proportions of the analyzed rocks are presented in Table 1. The granodiorite is equigranular and consists of plagioclase, biotite, K-feldspar and quartz with allanite, apatite, zircon, and ilmenite as accessory minerals. Some granodiorite samples are dominated by closely packed plagioclase (GD31, GD55, Fig. 3a) whereas other granodiorite samples are characterized by randomly distributed plagioclase grains with abundant interstitial K-feldspar (GD15, GD16, Fig. 3b). These granodiorites are termed cumulate (GD31, GD55) and non-cumulate (GD15, GD16), respectively.

Diorites and quartz diorites contain hornblende, plagioclase, biotite and quartz with accessory titanite, ilmenite, apatite, and zircon. Their texture varies from porphyritic (D10, D27) to serial (D30). Samples with porphyritic texture include large (up to 8 mm) biotite grains often enclosing numerous small plagioclase laths (Fig. 3c). Thin (1–5 mm) leucocratic veins, composed mainly of biotite, plagioclase, and quartz, crosscut some diorite samples (e.g., D10).

Quartz dioritic enclaves have mineral compositions similar to the massive diorites and quartz diorites (E48), but some have rims where biotite is the only mafic phase (E32). Thin (1–5 mm) leucocratic veins, composed mainly of plagioclase and quartz, crosscut enclave samples.

No significant alteration products were observed in diorites and enclaves; plagioclase is very rarely sericitized and rare chlorite occurs along hornblende and biotite cleavage.

The leucocratic vein (LV42) is composed of plagioclase, K-feldspar, muscovite, biotite, and quartz (Fig. 3d). It is sometimes strongly altered, porous and sheared in places. Biotite and muscovite are often chloritized and subsolidus sillimanite occurs rarely along shear zones in biotite.

Geochemistry

The major, trace element, and isotope composition of diorites and granodiorites are presented in Tables 2 and 3. The major and trace element composition for diorites D30 and D27 and isotope ratios for diorite D30 are presented in Pietranik and Waight (2008; Table 2 D30 is FGD1 and D27 is FGD2). Diorites (both massive diorites and enclaves) have SiO_2 and MgO contents that are often linearly correlated with other major and trace elements (Fig. 4). For example MgO correlates negatively with SiO_2 ($R^2 = 0.95$) and Rb ($R^2 = 0.69$) and positively with FeO ($R^2 = 0.75$), CaO ($R^2 = 0.92$), V ($R^2 = 0.81$), Sr ($R^2 = 0.76$), Y ($R^2 = 0.71$), MREE and HREE ($R^2 = 0.60$–0.75). All diorites have similar REE patterns with slight LREE

Table 1 Major and trace element concentrations in massive diorites (D), dioritic enclaves (E), granodiorites (GD) and leucocratic veins (LV) from the Gęsiniec Intrusion

	LV42	GD15a	GD15	GD16	GD55	GD31	E32	E48	D27	D10	D10a
SiO_2	72.8	64.2	65.2	64.5	59.5	59.8	59.6	56.00	57.8	51.40	54
TiO_2	0.5	0.7	0.7	0.7	0.9	1	1.2	1.40	0.8	1.90	1.5
A_2O_3	15.4	17.5	17.2	17.1	19.5	19.3	16.3	17.10	17.9	17.40	17.4
Fe_2O_3	1.1	4.2	4.8	4.5	4.6	4.8	7.5	8.20	7.3	10.40	8.7
MnO	0	0.1	0.1	0.1	0.1	0.1	0.1	0.10	0.1	0.20	0.1
MgO	1	1.3	1.3	1.3	1.2	1.6	3	3.60	3.4	4.10	4
CaO	0.2	4.2	3.9	4	4.8	5.2	5	6.80	6.4	7.80	7
Na_2O	3.9	4.1	3.9	3.9	4.3	4.8	3.1	3.20	3.3	3.50	3.2
K_2O	4.2	2.8	2.8	2.8	2.3	1.8	2.4	1.80	1.8	1.90	2.1
P_2O_5	0.2	0.3	0.2	0.3	0.3	0.4	0.4	0.50	0.6	0.90	0.6
Total	99.3	99.3	100.1	98.9	97.4	98.8	98.6	98.7	99.3	99.3	98.7
Sc			7	8	7	4	14	19		21	17
V			44	49	47	77	125	152		165	151
Cr			7				30	23		23	100
Ni			5	4	23	8	37	35		26	28
Cu			5	61	67	46	69	25		34	66
Rb			112	97	93	83	102	72		66	71
Sr			282	274	410	390	283	337		368	397
Y			22	21	16	17	32	42		49	39
Zr			429		613	777	284	254		254	254
Nb			21	18	21	25	27	35		41	33
Cs			2	2	3	1	2	1		1	1
Ba			894	721	1,109	766	732	712		587	504
La			96.2	79.4	26.2	46.2	34.7	58.2		51.1	36.1
Ce			170.1	154.8	53.5	83.4	77.3	116.9		118.5	88.2
Pr			18.9	16.9	6.4	8.4	9.9	13.6		16.0	12.1
Nd			60.1	60.4	26.6	28.9	38.7	48.7		61.0	50.3
Sm			9.0	8.5	4.2	3.9	7.1	9.0		11.8	9.3
Eu			1.5	1.5	1.6	1.7	1.6	2.0		2.6	2.3
Gd			8.6	6.0	3.8	2.9	5.8	8.8		11.1	8.4
Tb			0.9	0.8	0.5	0.5	1.0	1.3		1.6	1.4
Dy			4.4	4.3	2.8	2.7	5.8	6.9		8.7	7.5
Ho			0.7	0.7	0.6	0.6	1.1	1.4		1.7	1.4
Er			2.0	2.0	1.6	1.9	3.2	3.7		3.5	3.8
Tm			0.3	0.3	0.3	0.3	0.5	0.5		0.6	0.6
Yb			1.6	2.0	1.6	2.1	3.1	3.3		3.8	3.7
Lu			0.2	0.3	0.3	0.4	0.5	0.5		0.6	0.5
Hf			10	10	15	19	7	7		7	7
Ta			1	1	1	2	2	2		2	2
Pb			11	3	1	2	1	7		7	1
Th			21	21	5	11	4	6		1	2
U			3	4	2	3	3	2		1	1
Eu anomaly				0.65	1.24	1.56	0.76	0.7		0.68	0.77
La/Yb_{CHUR}				27.8	11	15.2	7.9	12.3		9.3	6.8

Eu anomaly ($Eu/\sqrt{Sm * Gd}$) and La/Yb_{CHUR} values were calculated using chondrite normalized values from Anders and Grevesse (1989)

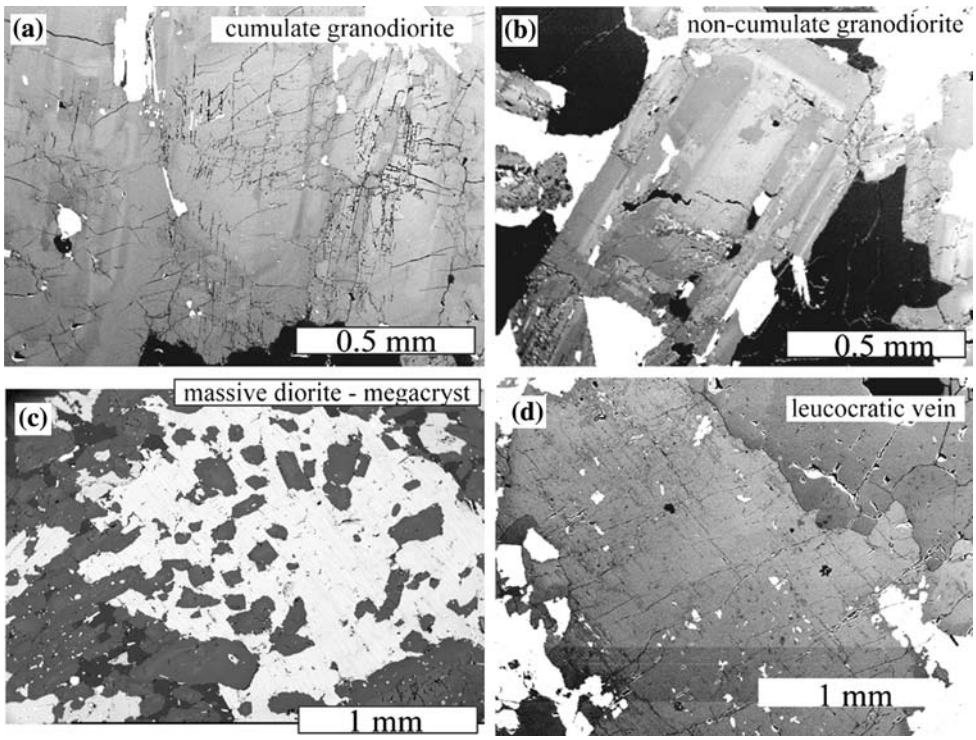

Fig. 3 BSE images of **a** closely spaced plagioclase grains in cumulate granodiorite, **b** plagioclase in non-cumulate granodiorite with larger amounts of interstitial minerals, **c** large poikilitic grain of biotite in quartz dioritic sample and **d** plagioclase in leucocratic vein

Table 2 Summary of petrography and mineral chemistry in diorites, dioritic enclaves and granodiorites from the Gęsiniec Intrusion

	Structure	Major minerals (modal proportions)	Plag (An %)	Hbl (#Fe, Al_{TOT}), Bt (#Fe, Al_{TOT})
Diorite D30	Euhedral Plag laths (0.25–2 mm long), euhedral to subhedral Hbl (0.25–0.8 mm), anhedral Bt (up to 0.8 mm) and interstitial Qzt (up to 0.6 mm)	Plag (50–52), Hbl (30–33), Bt (10–12), Qzt (6–7)	34–56	#Fe Hbl: 0.43–0.51%, Al_{TOT} Hbl: 1.5–1.9 apfu #Fe Bt: 0.53–0.61% Al_{TOT} Bt: 2.7–2.9 apfu
Diorite D10	Finer grained Plag and Hbl (from 0.1 to 0.5 mm) crosscut by coarser grained veins (0.5–5 mm) composed of poikilitic Bt, Qzt and Plag	Plag (47–49), Hbl (24–26), Bt (18–20), Qzt (10–11)	15–65	#Fe Hbl: 0.31–0.51%, Al_{TOT} Hbl:1.5–2.0 apfu #Fe Bt: 0.50–0.56% Al_{TOT} Bt: 2.6–2.7 apfu
Diorite D27	Medium grained (0.25–1.5 mm) with larger (up to 3 mm) Bt phenocrysts scattered throughout the rock	Pl (40–41), Hbl (20–22), Bt (19–20), Qzt (18–19)	31–62	#Fe Hbl 0.47–0.51% Al_{TOT} Hbl: 1.5–1.9 apfu, #Fe Bt: 0.50–0.58% Al_{TOT} Bt: 2.6–2.8 apfu,
Dioritic enclave E32	Rims impoverished in hornblende, domains composed of Plag, Hbl, Bt and Qzt with grain size of 0.25–1 mm crosscut by coarser grained veins (up to 3 mm) composed of Qzt, Plag and scarce Bt.	Pl (34–36), Hbl (24–26), Bt (18–20), Qzt (10–11)	20–60	#Fe Bt: 0.53–0.58% Al_{TOT} Bt: 2.4–2.5 apfu
Cumulate granodiorite D31, D55	Grainsize from 0.2–3 mm, dominates euhedral, closely spaced plagioclase	Pl (65), Bt(12), Kfds(10), Qzt (13)	20–53	#Fe Bt: 0.53–0.58% Al_{TOT} Bt: 2.7–2.9 apfu

enrichment (La/Lu_N = 7–12) and negative Eu anomalies (Eu/Eu* = 0.66–0.77, Fig. 5; Table 2).

The cumulate granodiorite is characterized by slight LREE enrichment (La/Lu_N = 9–13) and positive Eu anomalies (Eu/Eu* = 1.24–1.56) and it has the highest Sr contents (Table 2; Fig. 5).

The non-cumulate granodiorite is characterized by strong LREE enrichment (La/Lu_N = 26–41) and negative Eu anomalies (Eu/Eu* = 0.52–0.65; Table 2; Fig. 5).

The granodiorites tend to have lower MgO, FeO, TiO_2, P_2O_5, Ni, Cr, Y, V, Sc, Nb, Ta and HREE and higher SiO_2, and Th contents than the diorites (Table 2). The dioritic

Table 3 Rb–Sr and Sm–Nd isotopic data diorites and granodiorite from the Gęsiniec Intrusion

Sample	$^{87}Sr/^{86}Sr$	2 SE %	Rb (ppm)	Sr (ppm)	$^{87}Rb/^{86}Sr$	$^{143}Nd/^{144}Nd$	Sm (ppm)	Nd (ppm)	$^{147}Sm/^{144}Nd$	$(^{87}Sr/^{86}Sr)_{295}$	εNd_{295}
Diorite D33	0.71049	0.0011	73.4	327.4	0.6940	0.51232	9.0	49.1	0.111310	0.70778	−2.92
Enclave D48	0.70964	0.0010	64.0	328.1	0.5831	0.51231	9.0	49.3	0.110187	0.70720	−3.14
Granodiorite	0.71197	0.002	95.1	265.1	1.0382	0.51224	9.4	64.7	0.087713	0.70763	−3.73

Measured standard materials were $^{87}Sr/^{86}Sr = 0.710233 \pm 28$ (2σ) for NBS987 ($n = 11$), $^{87}Rb/^{85}Rb = 0.3857 \pm 3$ (2σ) for natural Rb solution ($n = 17$). Rb, Sr, Sm and Nd concentrations were measured by isotope dilution. Details of measurements are given in Pietranik and Waight (2008)

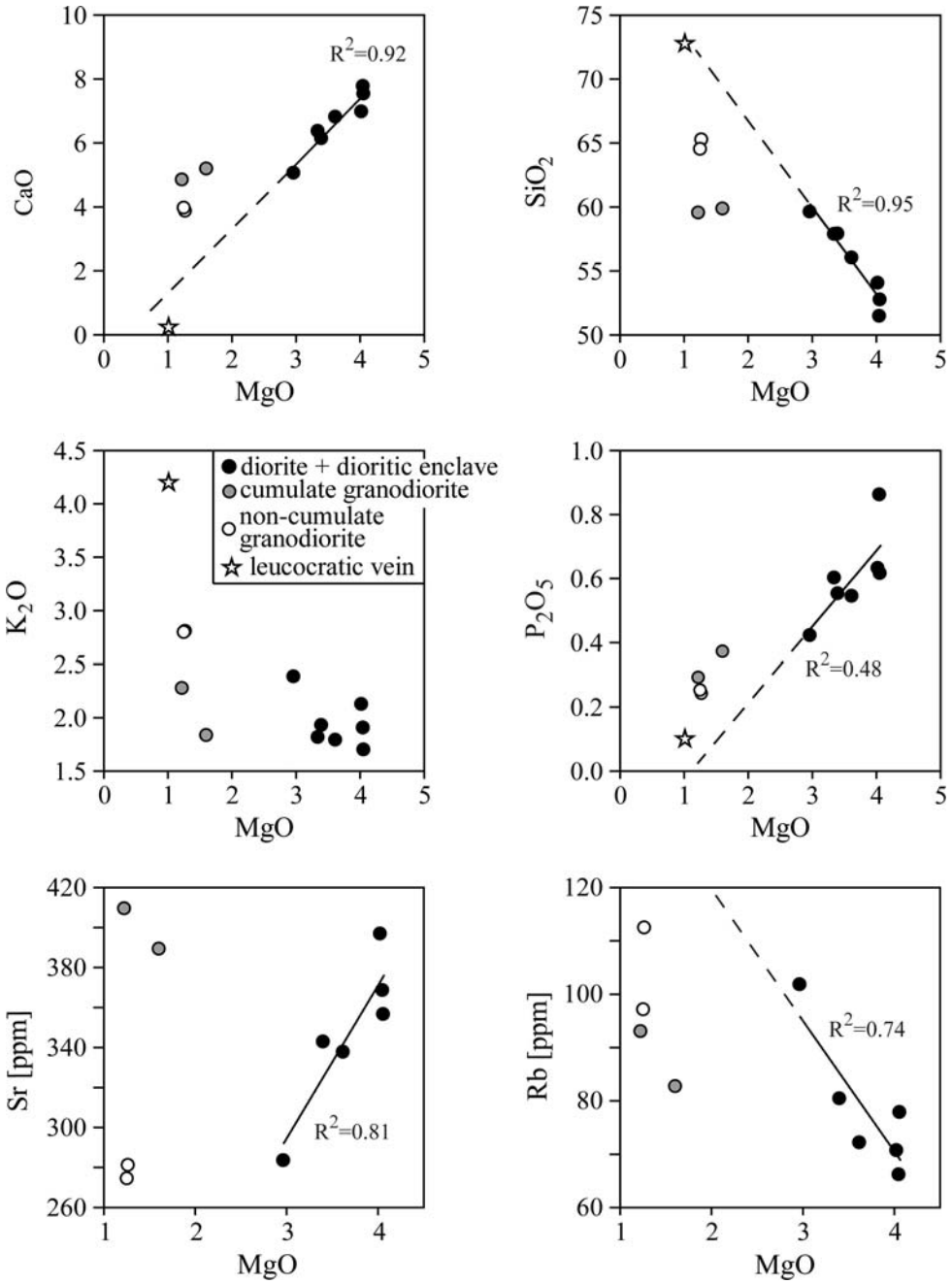

Fig. 4 Major and minor element geochemistry. The *solid lines* are regressions through all the dioritic and enclave samples with corresponding R^2 value

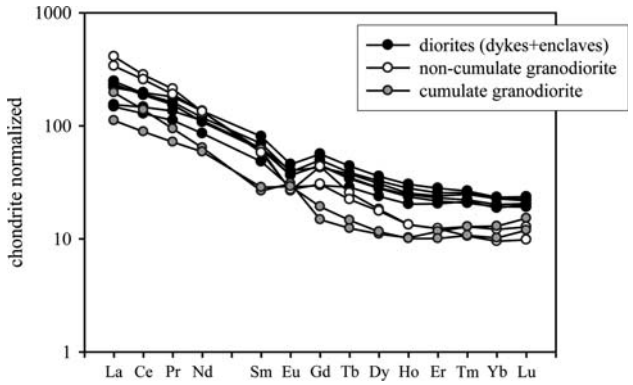

Fig. 5 REE and trace element compositions, with the REE patterns are normalized to chondrite (normalizing values from Anders and Grevesse 1989)

compositions only rarely trend towards granodioritic compositions and more often towards the composition of the leucocratic vein LV42 that crosscuts diorites (Fig. 4).

The lowest initial $^{87}Sr/^{86}Sr_{295}$ of 0.7069 and the highest initial ε_{Nd} of −3.2 occur in massive diorite D30 (Pietranik and Waight 2008). The initial isotopes of the other dioritic and enclave samples yield higher $^{87}Sr/^{86}Sr_{295}$ of 0.7072–0.7078 and lower initial ε_{Nd} from −2.9 to −3.1 (Table 3). The isotopic compositions of the granodiorite are $^{87}Sr/^{86}Sr_{295} = 0.7076$ and $\varepsilon_{Nd} = -3.7$ (Table 3).

Mineral chemistry

The chemical analyses of the minerals are presented in Supplementary Material (Table SM1).

Plagioclase

The plagioclase zonation and compositions are different in the granodiorites and diorites (Figs. 6, 7, 8).

Plagioclase from granodiorite

Plagioclase from the cumulate granodiorite (GD31, GD55) has slightly embayed, normally zoned cores ($An_{52–35}$) surrounded by a zone ($An_{50–35}$) characterized by multiple resorption surfaces and rims of $An_{35–23}$ (Fig. 6a). The zonation patterns are similar in cumulate and non-cumulate granodiorite samples. Detailed descriptions of plagioclase from non-cumulate granodiorite (GD15, GD16) were presented in Pietranik et al. (2006), although at least part of the embayed cores are now thought to have formed before the zones characterized by multiple resorption, since the multiple resorption surfaces mimic the shape of the embayed cores (Fig. 6b). The maximum An contents are similar in GD15 and GD31 ~ $An_{50–52}$ (Fig. 7a) while occurring in the central parts of the plagioclase, but much lower in GD55 (~$An_{37–38}$), while occurring in the resorption zones. The minimum An content (An_{min}) is defined as the lowest An content for which abundant analyses of plagioclase were measured: in other words, between the An_{min} and any lower An content measured in plagioclase in an individual sample, the number of analyses decreases at least a factor of 3 (Fig. 7; Table 4). The An_{min} is $An_{28–30}$ for GD15, $An_{26–28}$ GD55, and $An_{30–32}$ for GD31 (Table 4).

Plagioclase from diorite

Plagioclase from diorite and quartz diorite has strongly embayed cores ($An_{65–50}$) that are surrounded by $An_{50–34}$ plagioclase. The embayments are filled by plagioclase with similar An content to that in the surrounding plagioclase and also by hornblende and biotite (Fig. 6c, d). The zonation patterns as well as the range of An and Or composition are similar in plagioclase from different samples of diorites, quartz diorites, and enclaves (Figs. 6c, d, 7b). The An_{min} are strikingly similar in all plagioclase grains from an individual diorite or enclave sample and between most dioritic and enclave samples ($An_{34–36}$) (Fig. 7b; Table 4); the only exception is massive diorite D27 with higher An_{min} of $An_{38–40}$. The maximum anorthite contents ($An_{65–57}$) differ slightly from sample to sample (Table 1), but that may be due to sampling strongly embayed cores that do not record the full range of initial An composition.

Comparison of the plagioclase from the granodiorites and diorites (dykes and enclaves) shows that the latter have higher maximum and minimum An contents and they tend to have lower Or contents for a given An content (Fig. 7c).

Sr concentration in plagioclase

We have used the Sr concentration in plagioclase to calculate the concentration in the melt using the partition coefficients of Bindeman et al. (1998). Such an approach allows interpretation of the change in Sr concentration in plagioclase in terms of contemporaneous changes in melt composition. The results are shown in Fig. 8 and the limitations of this approach are discussed in Appendix.

All the granodiorites yield similar maximum Sr values in the melt for the plagioclase cores despite differences in their An contents (Fig. 8a), whereas the minimum Sr values in the melt are higher for the cumulate granodiorites (Fig. 8a). Plagioclase crystallizing after resorptions is enriched with Sr (Fig. 8a) in both the cumulate and the non-cumulate granodiorite (Pietranik et al. 2006).

All diorites and enclaves yield similar An versus Sr in the melt arrays which can be subdivided into two, broadly linear trends: a steeper one for $An_{65–45}$ comprising analyses

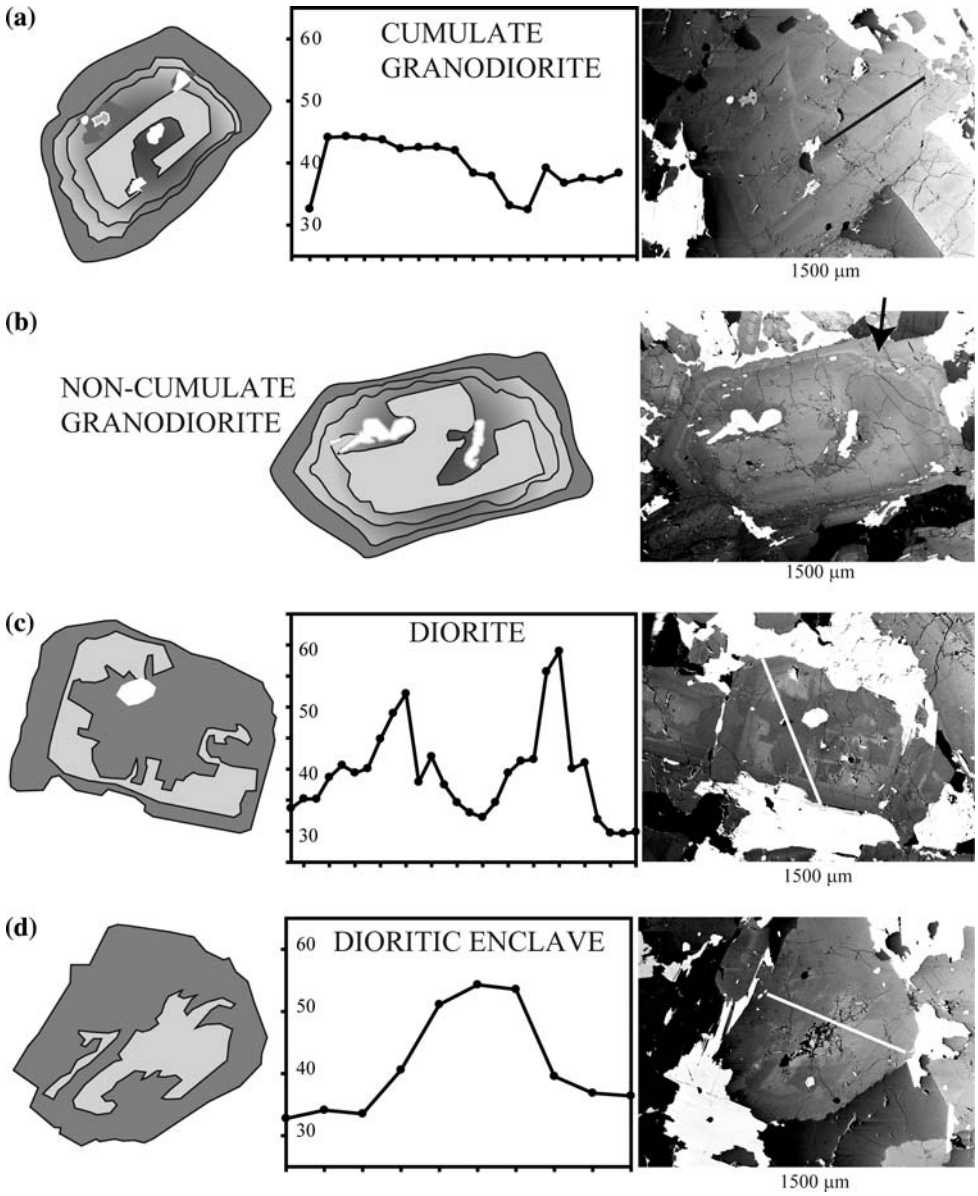

Fig. 6 Schematic zonation of plagioclase from **a** cumulate granodiorite, **b** non-cumulate granodiorite, **c** diorite, and **d** a dioritic enclave with an exemplary BSE image and corresponding An traverse. The *arrow* in the BSE image of plagioclase from the non-cumulate granodiorite (**b**) indicates where the outer resorption surface mimics the shape of an already embayed core suggesting that embayment happened before this resorption

of embayed cores (trend 1), and a shallower one for $An_{45–32}$ (trend 2) comprising outer parts of embayed cores, rims and plagioclase from embayments (Fig. 8b). There is a slight increase in Sr content from trend 1 to trend 2 at similar An.

Biotite

Biotites in all the diorite, dioritic enclave, and cumulate granodiorite samples have overlapping Al^{TOT} a pfu and Ti a pfu contents (Fig. 9). Biotite in non-cumulate granodiorite has higher Fe/(Fe + Mg) ratios than those in diorite and cumulate granodiorite, and overlapping Al^{TOT}, Ti a pfu contents (Fig. 9). Biotite in the leucocratic vein has lower Fe/(Fe + Mg) ratios and Ti a pfu contents and higher Al^{TOT} a pfu compared to all other samples (Fig. 9).

Discussion

Origin of the geochemical and mineralogical variations in the dioritic-granodioritic suite

The petrological and geochemical characteristics of mingled dioritic and granodioritic to granitic magmas often include the same features, common to many outcrops worldwide (e.g., Dorais et al. 1990; Didier and Barbarin 1991; Pitcher 1993; Elburg 1996; Wiebe et al. 1997; Altherr et al. 1999; Waight et al. 2001; Janoušek et al. 2004; Tepper and Kuehner 2004; Kumar and Rino 2006). The more mafic magmas are usually finer grained and chilled against the more felsic host. They contain abundant acicular apatite, and zoned plagioclase, often with bimodal

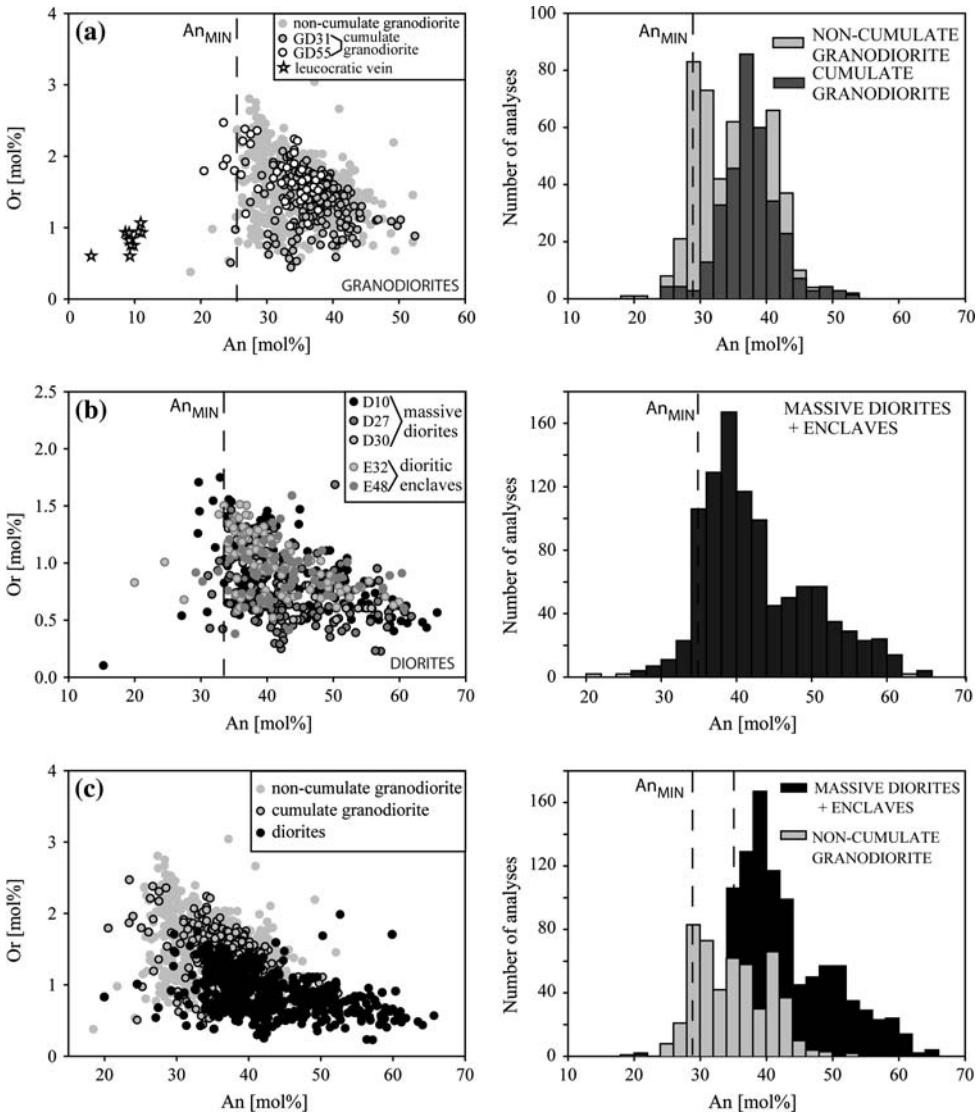

Fig. 7 An versus Or content in plagioclase (*left-hand side*) and corresponding histograms of An (bin width 2 mol%, *right-hand side*) for **a** granodiorite, **b** diorite and dioritic enclaves and **c** all samples. *Dashed lines* show An_{min} values. Note that An_{min} is not defined for cumulate granodiorite

distributions of anorthite content (e.g., Elburg 1996; Janoušek et al. 2004). Plagioclase and K-feldspar megacrysts typical of the more felsic magma are found within mafic enclaves suggesting mechanical transfer of the crystals between two magmas (Elburg 1996; Waight et al. 2000; Słaby et al. 2008; Vernon and Paterson 2008). Enclaves often have mineralogy and compositions of minerals similar to those in the host (Tepper and Kuehner 2004). The major and minor element contents of both magmas commonly form linear trends when plotted against differentiation indexes such as SiO_2 or MgO, although similar relationships are not always observed for trace elements (e.g., Elburg 1996; Kumar and Rino 2006). Mafic rocks and enclaves usually have lower $^{87}Sr/^{86}Sr$ ratios and higher εNd than the felsic host, but the compositional fields often overlap (e.g., Elburg 1996; Altherr et al. 1999; Waight et al. 2007), which may be partly due to diffusional re-equilibration (e.g., Pin et al. 1990).

Models constraining the compositional evolution of both the mafic magmas and the felsic host have to take all these features into account. The presently accepted models usually comprise two stages. The first stage is envisioned as a stratified magma chamber with more mafic magma residing at the bottom (e.g., Elburg 1996; Wiebe 1996; Janoušek et al. 2004; Tepper and Kuehner 2004; Kumar and Rino 2006), and it includes (a) formation of hybrid magma at the boundary between felsic and mafic magmas by mixing with or without crystal transfer between the two magmas (e.g., Kumar and Rino 2006), and/or (b) melt–melt diffusion driven chemical exchange leading to formation of hybrid magma with trace element contents and isotopic ratios in equilibrium with both melts (e.g., Tepper and Kuehner 2004). Alternatively, some of the compositional variability in both magmas is attributed to mixing between the magmas in composite dykes en route to magma chamber (Collins et al. 2000) or to earlier fractionation-mixing-

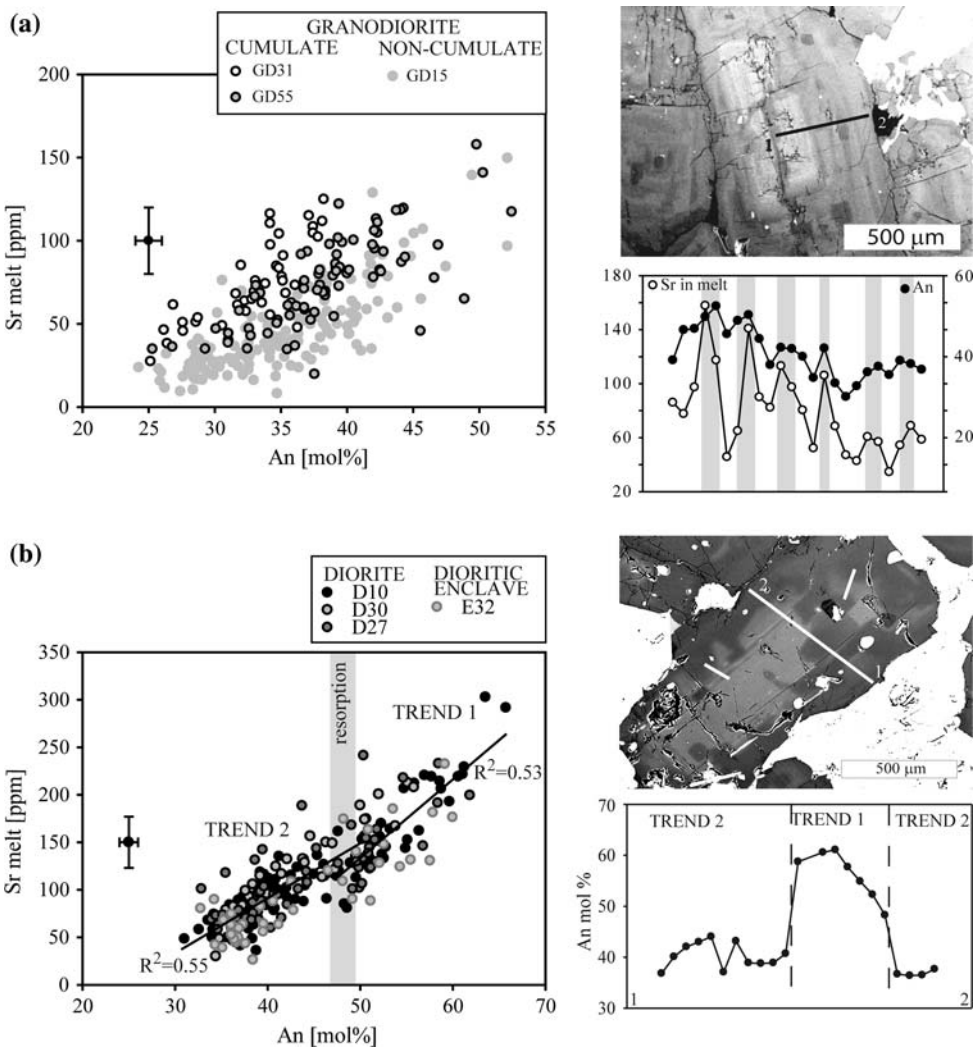

Fig. 8 A plot of An versus Sr in the melt in equilibrium with plagioclase for **a** granodiorite and **b** diorite samples. BSE images and corresponding An and Sr in the melt, traverses are shown for representative plagioclase grains. Note that the plagioclase grain from the cumulate granodiorite has a cracked core and a complex rim with multiple resorption surfaces. *Gray bands* mark increases in An content that correspond to the plagioclase that crystallized after resorptions with accompanying increases in Sr in the melt contents. Trend 1 and Trend 2 are regressions through plagioclase data before and after resorptions, respectively

assimilation processes that took place before the magmas came into contact (e.g., Pitcher 1993; Tepper and Kuehner 2004). The second stage commences after intrusion of more mafic magma into the overlying host either as syn-plutonic dykes or in response to convection; hybridized mafic enclaves are hence dispersed within the host. This stage includes equilibration either by residual melts or sub-solidus fluids and it is often thought to be responsible for the similar chemistry of minerals in the host and the enclaves. It is typically assumed that processes of both stages contributed to compositional trends observed in the mafic magma; however, variations of major element chemistry are often explained by just the first stage of mafic–felsic magma mixing with subsequent formation of a range of hybridized magmas.

In the mixing models presented in the literature the amount of felsic magma required to produce a range of whole rock compositions similar to that observed in the massive diorites and enclaves in the Gęsniniec intrusion (roughly from 50 to 60% of SiO_2) is usually ~10–70% (e.g., Elburg 1996; Janoušek et al. 2004; Kumar and Rino 2006). If we assume that similar processes led to the chemical diversity of the Gęsiniec enclaves and syn-plutonic dykes and choose the non-cumulate granodiorite GD15 (with a negative Eu anomaly) as the felsic member and the most isotopically primitive diorite D30 as the mafic end member, the rough proportion of granodioritic magma required to produce the observed compositional range in the diorites would be similar (~10–50%, Table 5). Even if the non-cumulate granodiorite is not the perfect candidate for the felsic end-member in the Gęsiniec Intrusion, it provides a good approximation of the proportions of felsic melt required to hybridize the dioritic magmas. However, if the dioritic to quartz dioritic rocks are in fact hybrids containing as much as 50% of granodioritic (or other felsic) melt, the hybridization process between two such chemically different magmas should have been recorded in the composition of minerals that crystallized during hybridization.

Most of the rock-forming and accessory minerals are thought to have equilibrated with late-stage melts or fluids,

Table 4 Data for An histograms

An	D10	D27	D30	E32	E48	All diorites	GD15	GD31	GD55
19	1	0	0	0	0	1	1	0	0
21	0	0	0	1	0	1	1	0	1
23	0	0	0	0	0	0	0	0	3
25	0	0	0	1	0	1	8	3	1
27	1	0	0	1	0	2	21	3	*6*
29	3	0	0	0	1	4	*83*	2	2
31	2	1	0	0	1	6	73	*9*	5
33	5	3	1	2	1	11	42	23	7
35	*20*	7	*7*	*16*	*4*	*53*	62	32	14
37	28	4	7	22	6	67	58	60	11
39	36	*16*	13	18	9	86	30	42	2
41	21	14	6	8	8	60	66	24	0
43	12	13	5	9	11	52	37	16	0
45	5	6	5	1	5	21	10	5	0
47	11	3	3	2	4	27	4	2	0
49	7	7	5	7	4	30	3	3	0
51	5	15	5	3	2	29	0	2	0
53	9	3	3	4	1	18	2	1	0
55	7	3	6	2	1	15	0	0	0
57	3	4	0	2	1	12	0	0	0
59	6	3	0	2	2	13	0	0	0
61	4	1	0	0	2	8	0	0	0
63	1	0	0	0	0	1	0	0	0
65	2	0	0	0	0	2	0	0	0
67	0	0	0	0	0	0	0	0	0
Analyzes[a]	189	103	66	101	63	552	501	227	52
Grains[b]	7	6	5	7	3	26	18	4	9

Cells with values representing An_{min} are in *italic*

Numbers in An column are An values for the bin center in histograms of An, each bin is 2 mol%

[a] Number of microprobe spots analyzed in plagioclase

[b] Number of plagioclase grains analyzed in each sample

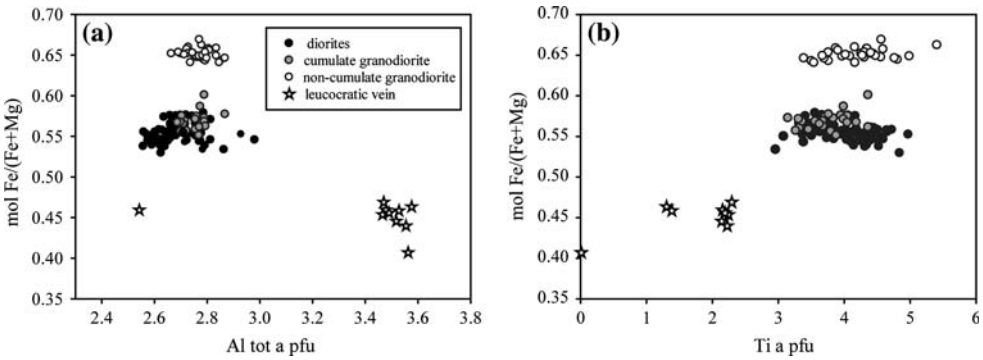

Fig. 9 Comparison of biotite compositions in dioritic and granodioritic rocks

after the mafic magma was entrained as enclaves into the felsic host (Tepper and Kuehner 2004). Plagioclase is thought to be the only mineral that may preserve its original composition, and very often plagioclase from enclaves has higher An contents than plagioclase in the host (e.g., Janoušek et al. 2004; Tepper and Kuehner 2004; Kocak 2006). Therefore, we evaluate the plagioclase morphological and compositional zonations to see if they preserve a record of mixing between felsic and mafic magmas.

Record in granodioritic plagioclase

Plagioclase from felsic rocks often shows numerous resorption zones formed in response to injections of mafic magma into the felsic magma chamber with subsequent homogenization and hybridization (e.g., Hattori and Sato 1996; Tepley et al. 2000; Waight et al. 2000). A similar conclusion was reached for the non-cumulate Gęsiniec granodiorite on the basis of multiple resorption zones surrounded by plagioclase with higher An and Sr contents

Table 5 Least square mass balance calculations

(a)	GD15	D30	Model	D10	Model	E48	Model	D33	Model	E32
SiO_2	64.5	52.7	54	54	55.8	56	57.5	57.9	59.3	59.6
TiO_2	0.7	1.6	1.5	1.5	1.4	1.4	1.2	1.3	1.1	1.2
Al_2O_3	17.1	17.6	17.5	17.4	17.4	17.1	17.4	16.5	17.3	16.3
Fe_2O_3	4.5	9.3	8.8	8.7	8.1	8.2	7.3	7.7	6.6	7.5
MnO	0.1	0.2	0.2	0.1	0.1	0.1	0.1	0.1	0.1	0.1
MgO	1.3	4.1	3.7	4	3.3	3.6	2.9	3.4	2.5	3
CaO	4	7.5	7.1	7	6.6	6.8	6.1	6.1	5.5	5
Na_2O	3.9	3.2	3.3	3.2	3.4	3.2	3.5	2.9	3.6	3.1
K_2O	2.8	1.7	1.8	2.1	2	1.8	2.1	1.9	2.3	2.4
P_2O_5	0.3	0.6	0.6	0.6	0.5	0.5	0.5	0.6	0.4	0.4
GD15%			11%		26%		41%		56%	
D30%			89%		74%		59%		44%	
Σr^2			0.23		0.35		1.8		2.67	

(b)	GD31	LV42	Model	GD15
SiO_2	59.8	72.8	64.3	64.5
TiO_2	1	0.5	0.8	0.7
Al_2O_3	19.3	15.4	18	17.1
Fe_2O_3	4.8	1.1	3.5	4.5
MnO	0.1	0	0	0.1
MgO	1.6	1	1.4	1.3
CaO	5.2	0.2	3.5	4
Na_2O	4.8	3.9	4.5	3.9
K_2O	1.8	4.2	2.7	2.8
P_2O_5	0.4	0.2	0.3	0.3
GD31%			65%	
LV42%			35%	
Σr^2			2.5	

(c)	LV	D30	Model	D10	Model	E48	Model	D33	Model	E32
SiO_2	72.8	52.7	54.1	54	55.8	56	57.5	57.9	59.3	59.6
TiO_2	0.5	1.6	1.5	1.5	1.4	1.4	1.3	1.3	1.2	1.2
Al_2O_3	15.4	17.6	17.4	17.4	17.2	17.1	17	16.5	16.9	16.3
Fe_2O_3	1.1	9.3	8.8	8.7	8.1	8.2	7.3	7.7	6.6	7.5
MnO	0	0.2	0.2	0.1	0.1	0.1	0.1	0.1	0.1	0.1
MgO	1	4.1	3.9	4	3.6	3.6	3.3	3.4	3.1	3
CaO	0.2	7.5	7	7	6.4	6.8	5.8	6.1	5.1	5
Na_2O	3.9	3.2	3.2	3.2	3.3	3.2	3.4	2.9	3.4	3.1
K_2O	4.2	1.7	1.9	2.1	2.1	1.8	2.3	1.9	2.5	2.4
P_2O_5	0.2	0.6	0.6	0.6	0.6	0.5	0.5	0.6	0.5	0.4
LV%			7%		15%		24%		33%	
D30%			93%		85%		76%		67%	
Σr^2			0.08		0.33		1.09		1.39	

(a) Magma mixing between granodiorite and the least evolved diorite to produce range of dioritic compositions, *(b)* mixing between GD31 granodioritic cumulate and leucocratic vein to produce non-cumulatic granodioritic composition and *(c)* mixing between the leucocratic vein and the least evolved diorite to produce range of dioritic compositions using the program PETMIX (Wright and Doherty 1977)

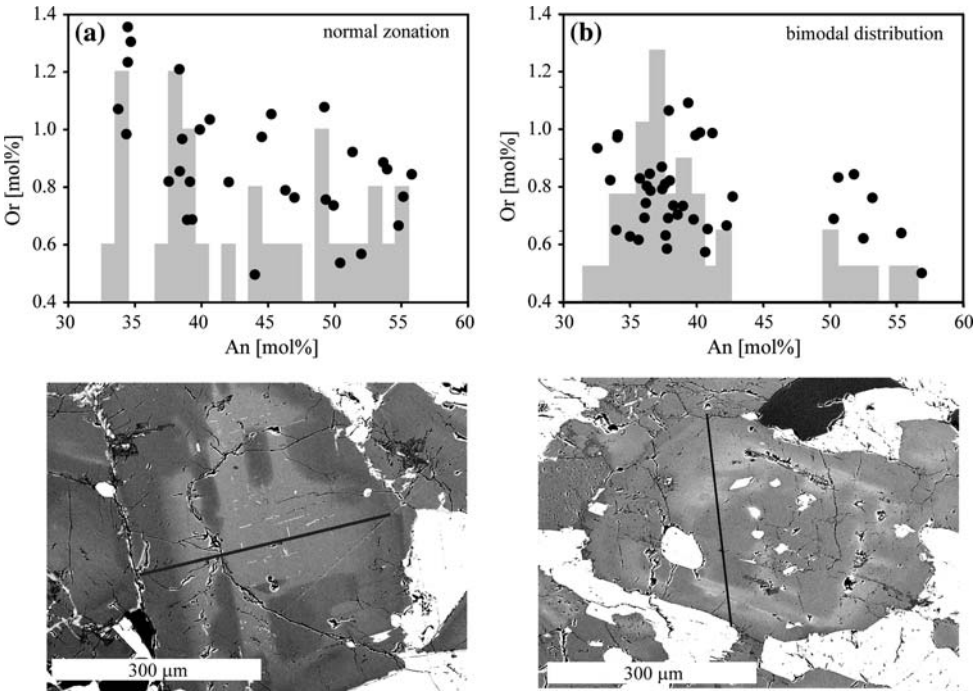

Fig. 10 A plot of An against Or content and An histograms in two plagioclase grains from dioritic samples with corresponding BSE images and microprobe traverses: **a** smooth change in An content from core to rim and **b** bimodal distribution of An content across a resorption zone

(Pietranik et al. 2006). Similar records of multiple resorption are preserved in both the non-cumulate and cumulate granodiorites (Fig. 6a, b) indicating that formation of plagioclase cumulates took place late during granodiorite crystallization, after mixing with presumably hotter and more mafic magmas. Therefore, three processes of magma differentiation can be deduced from the plagioclase compositions in the granodiorite: (1) crystallization of the inner parts of plagioclase in variable P-T-XH_2O conditions consistent with the different An contents in plagioclase cores in different samples (for example GD55 versus GD31 or GD15), but with similar Sr in the melt contents (Fig. 8a); (2) mixing, probably with dioritic magma, currently represented by enclaves and massive diorites, and (3) removal of late, evolved melts from some granodiorites to produce cumulate granodiorites.

Record in dioritic plagioclase

The record in the granodioritic plagioclase seems to corroborate the magma mixing model. However, is a similar record also preserved in the plagioclase crystals in the diorites? Plagioclase from dioritic to quartz dioritic rocks tends to be characterized by complex zonation and a bimodal An distribution. This is often cited as evidence for hybridization of mafic magma by a more felsic one, with the high An cores having originated in diorite magma and then resorbed after injection into a felsic magma chamber (e.g., Elburg 1996; Janoušek et al. 2004). However, we believe that magma mixing may not be required to explain the bimodal An distribution in the Gęsiniec diorites. Instead, we argue that it is a direct consequence of the plagioclase morphology developed in response to the resorption of the cores. In the Gęsiniec Intrusion, resorption occurred after at least 30% of the plagioclase had crystallized (estimated from the average area of euhedral cores before resorption as a percentage of the average area of the whole plagioclase grain), and it predominately affected the interiors of the cores, leaving in some cases, the outer portions intact. If a probe traverse across a plagioclase grain does not intersect any resorption surface, there will be no compositional gap and the An content decreases smoothly from core to rim (Fig. 10a). In contrast, if the traverse intersects a resorbed core it will yield bimodal An distribution, but only because plagioclase of intermediate compositions has been removed during resorption (Fig. 10b).

The central evidence against the resorption having been caused by mixing between dioritic and granodioritic magmas in the Gęsiniec Intrusion is the lack of change in plagioclase An_{min}, Or and Sr in the melt content between the massive diorite and enclave samples (Figs. 7b, 8b) that would reflect variable hybridization, even though there are substantial differences in the Or and An contents between the dioritic and granodioritic plagioclase (Fig. 7c). Even if plagioclase crystallization in the dioritic magmas started before mixing and from compositionally similar magmas, some variation in plagioclase composition and the compositional trends of An versus Or and Sr would be expected between the 90/10% and 50/50% mixtures of mafic and

felsic magmas (as estimated for the Gęsiniec Intrusion by rough mass balance calculations; Table 5), and yet none is observed.

The An content of dioritic plagioclase that crystallized after resorption is similar to, or lower, than that of the plagioclase that crystallized before resorption, which is not consistent with the resorption being due to increase in temperature or water content (e.g., Tsuchiyama 1985; Singh and Johannes 1996; Nakamura and Shimakita 1998). The geometry of the resorption surface, with its strongly embayed cores, and the lack of compositional change could be induced by decompression—similar resorption features are seen in the granodioritic plagioclase (Pietranik et al. 2006) and other dioritic rocks from the Gęsiniec Intrusion (Pietranik and Waight 2008). The latter are not in contact with granodiorite rocks and decompression-induced resorption is consistent with the constant Sr isotope ratios across an embayed resorption boundary (Pietranik and Waight 2008). If the ascending magma has high water contents it may reach water saturation on the way to the surface and decreasing water contents in the magma will induce crystallization of more albitic plagioclase, thus producing a rapid decrease in An content without a contribution from more felsic magma. Decreasing temperature, as during ascent and emplacement, will have a similar effect. Thus, we argue that plagioclase from dioritic rocks was resorbed most probably due to decompression and not due to magma mixing.

Magma mixing is also not required to explain the two trends in the An versus Sr in the melt diagram (Fig. 11). Rather the change in slope could be due to the resorption of the cores. Trend 1 in Fig. 11 can be modeled by 55% fractional crystallization of predominately plagioclase (~65%) and hornblende (~35%) followed by resorption of ~20% of the crystallized assemblage (i.e., ~10% of the whole rock) to produce the increase in Sr in the melt as observed between Trends 1 and 2 (Fig. 11). Trend 2 represents renewed crystallization after resorption of the plagioclase cores. As temperature and/or water contents should be lower, more minerals join the crystallizing assemblage and Trend 2 is attributed to 42% fractional crystallization of ~20–40% plagioclase and 60–80% of other minerals such as hornblende, biotite, quartz, K-feldspar, and accessories (see caption to Fig. 11). The amount of plagioclase that crystallized in the model is ~44%, consistent with its modal abundances in the diorites (Table 2). The amount of plagioclase that crystallized before resorption is ~30%, also in agreement with the volumes of unresorbed cores observed in thin sections. Modelling Trend 1 in terms of fractional crystallization of plagioclase and hornblende is also consistent with observations in thin sections where both plagioclase and hornblende are euhedral and thus close to liquidus phases.

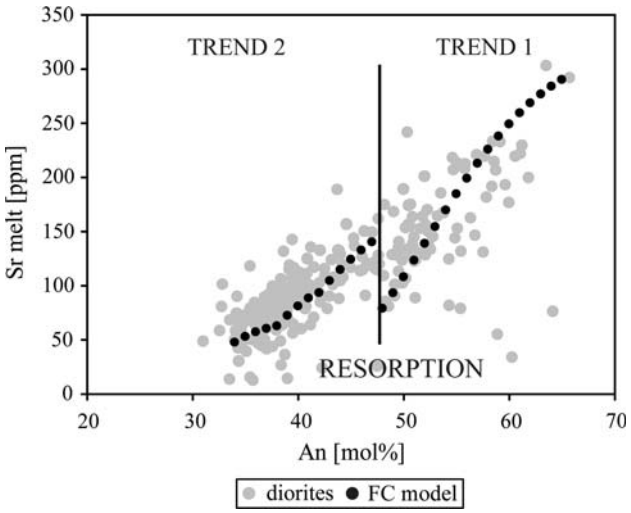

Fig. 11 Modelling the evolution of Sr in the melt during crystallization of dioritic plagioclase. The model assumes 1% decrease in An content with 3% of crystallization, and a similar dAn/dT was obtained in experiments on natural rocks (Prouteau and Scaillet 2003, on Mount Pinatubo dacite or Housh and Luhr 1991, on andesite compositions). The partition coefficients are from Bindeman et al. (1998) and they change with An content. Trend 1 is modeled by Raleigh's fractional crystallization of 65% of plagioclase and 35% of hornblende (partition coefficient for hornblende is taken to be 0.1, GERM database yields coefficients between 0.02 and 0.3, but using any coefficient from this range does not affect the model). The increase in Sr in the melt between Trends 1 and 2 is modeled by resorption of ~20% of the crystallized assemblage (65% Plag + 35% Hbl). Trend 2 is modeled by crystallization of 40–20% plagioclase (with decreasing proportion of plagioclase with each 5% of anorthite) to approximate for the appearance of other minerals as the temperature approaches the solidus. *Dots represent* ~3% of crystallization, and the total amount of plagioclase crystallized at the end of this trend is ~44% with ~90% of magma having crystallized

In summary, the chemical zoning in the dioritic plagioclase does not require hybridization of the dioritic magmas by felsic ones. Rather the observed An versus Or and Sr trends can be explained by fractional crystallization and resorption due to decompression during magma ascent. Similar compositions of plagioclase in all the dioritic samples indicate that probably no hybridization occurred before resorption and that the diorites analyzed represent a single batch of magma.

So, if all dioritic plagioclases record crystallization from chemically similar parental magma, what is the cause of the whole rock chemical variability in the diorites and quartz diorites? It is argued that the observed range of whole rock compositions was produced by close to the solidus, or subsolidus, interactions between the diorites and leucocratic melt squeezed from the granodiorite. This is supported by two lines of evidence:

(1) Mass balance calculations involving massive diorite (D30) and the leucocratic vein (LV42) produce a

range of dioritic compositions with lower residual errors than the same calculations for diorite and granodiorite (Table 5a, c). The residuals for the most evolved diorites and enclaves (D33, E32) are still large enough not to support a simple 2-component mixing. However, this is to be expected as the leucocratic melt squeezed from granodiorite would vary in composition and the variations were not easy to analyze in thin leucocratic veins.

(2) Increases in the biotite/hornblende ratio with increasing SiO_2 suggests close to solidus, or subsolidus, reaction of Hbl + K-rich melt/fluid to produce Bt + SiO_2, similar to reactions observed in other enclaves and dioritic rocks (e.g., Elburg 1996; Roberts et al. 2000). Such subsolidus reactions would also contribute to the variations in whole rocks compositions, potentially increasing the residuals in the mass balance calculations.

However, if the suggested interactions took place close to the solidus, how could the leucocratic melt have been distributed within the diorite without affecting the plagioclase compositions? A key point is that the amount of leucocratic melt needed to hybridize the dioritic samples is much lower than of the amount of granodioritic magma required. It is in the range ~7–33% (Table 5c), and the infiltration of the leucocratic melt might also have been localized as suggested by textures in dioritic samples (Fig. 12). The melt could have intruded solidified, or almost solidified, diorite and been distributed as thin veins. The melt was rich in potassium and this could have triggered the reaction Hbl → Bt described above. For example, large biotite poikilocrysts occur in Hbl-free, quartz rich veins in the sample D10, where the amount of the melt is small (Fig. 12), marking probable paths of the leucocratic melt injection. The distribution, size, and composition of plagioclase enclosed by the oikocrysts are similar to those in the Hbl-rich surroundings (Fig. 12, D10), suggesting that plagioclase was not affected by the infiltrating melt. When the proportion of leucocratic melt was larger, for example, ~33% in enclave E32 (Fig. 12), the melt was probably distributed interstitially through the rock volume initiating the reaction Hbl → Bt in the whole sample. Nonetheless, remnants of initial veins of the leucocratic material are still preserved (Fig. 12, indicated by arrows).

Overall, the compositional variations in the diorite samples may be explained by infiltration of the leucocratic melt during the late stages of diorite crystallization or shortly after its complete solidification.

In our preferred scenario of mafic–felsic magma interaction the dioritic magma in Gęsiniec was intruded into partially solidified granodiorite, and in view of the temperature contrast it formed dioritic sheets, disintegrated synplutonic dykes, or chilled separate blobs of magma (e.g., as proposed by Barbarin 2005). Injection of a dyke and heating of the granodiorite would trigger resorption in plagioclase in the granodiorite and facilitate separation of late melts that in turn interacted with diorites. Remelting of a mushy granitic body by injection of hot basaltic magma is consistent with field and petrological evidence in other intrusions (e.g., Wiebe et al. 2004). Therefore, the record in plagioclase from both the diorites and the granodiorites indicates interaction between partially (the granodiorite) or perhaps completely (the diorite) crystallized rocks after the magmas were emplaced.

Origin of granodioritic and dioritic magmas

Most hypotheses for the origins of magmas in mafic–felsic mingling zones assume two different sources for the mafic

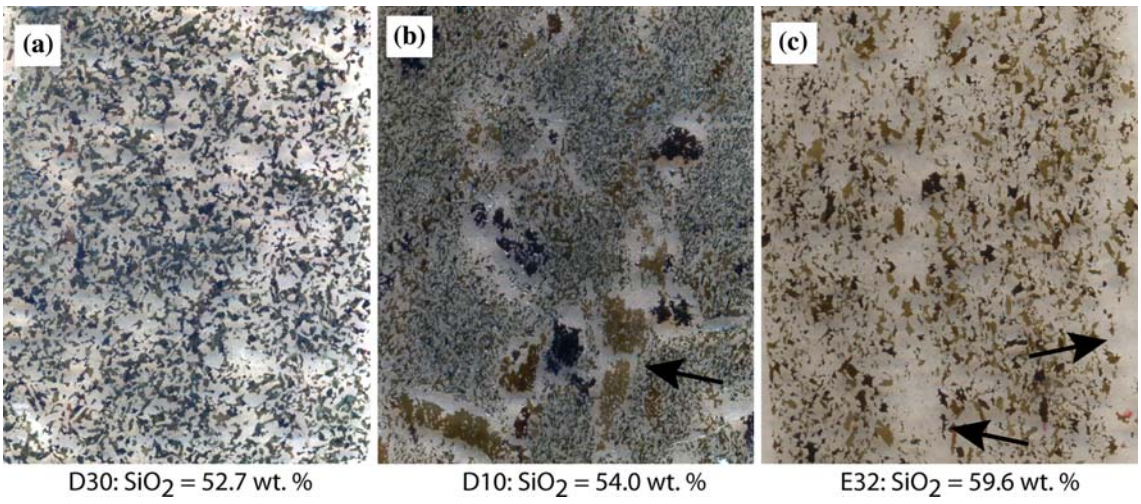

Fig. 12 Textures of dioritic samples showing different stages of hybridization. The bottom edge is approximately 1.5 cm

and felsic magmas, either the mantle and the crust or two different crustal sources. Another interpretation is that the dioritic enclaves are less evolved magmas related to the granodiorites by fractional crystallization (Donaire et al. 2005) or assimilation fractional crystallization. Derivation from different sources is often supported by the trace element contents, but not the isotope ratios. For example, the Gęsiniec diorites and granodiorite have overlapping Sr and Nd isotope compositions ($^{87}Sr/^{86}Sr_{init} = 0.7069–0.7078$ and $\varepsilon Nd = -2.9$ to -3.1 in the diorites and 0.7076 and -3.7 in the granodiorite). However, similar isotopic compositions between enclaves and host have been attributed to isotopic equilibration (e.g., Elburg 1996), which is more effective than geochemical equilibration (Lesher 1990). Distinct sources of the Gęsiniec diorites and granodiorites are supported by (a) different minor and trace element contents with the granodiorite having negative Ti, Nb and Ta anomalies that are not seen in the diorites (Białek and Pietranik 2006) and (b) different An versus Or and An versus Sr trends in plagioclase from granodiorites and diorites (Fig. 7).

The infiltration of late-stage melts into the Gęsiniec diorite was probably responsible for an increase in the Sr isotope ratios from those in the least-evolved diorites (e.g., D30 = 0.7069) to those in the more contaminated samples (e.g., D33 = 0.7078). The least-evolved sample (D30) shows no textural features indicative of contamination by late-stage melts (Fig. 12), and similar plagioclase zonation and compositions in all the dioritic samples suggest a similar crystallization history for all diorites before emplacement. In addition, the granodioritic plagioclase in the Gęsiniec Intrusion records magma mixing only at a late stage, and the earlier part of its crystallization history appears to be similar to that of plagioclase in the diorites

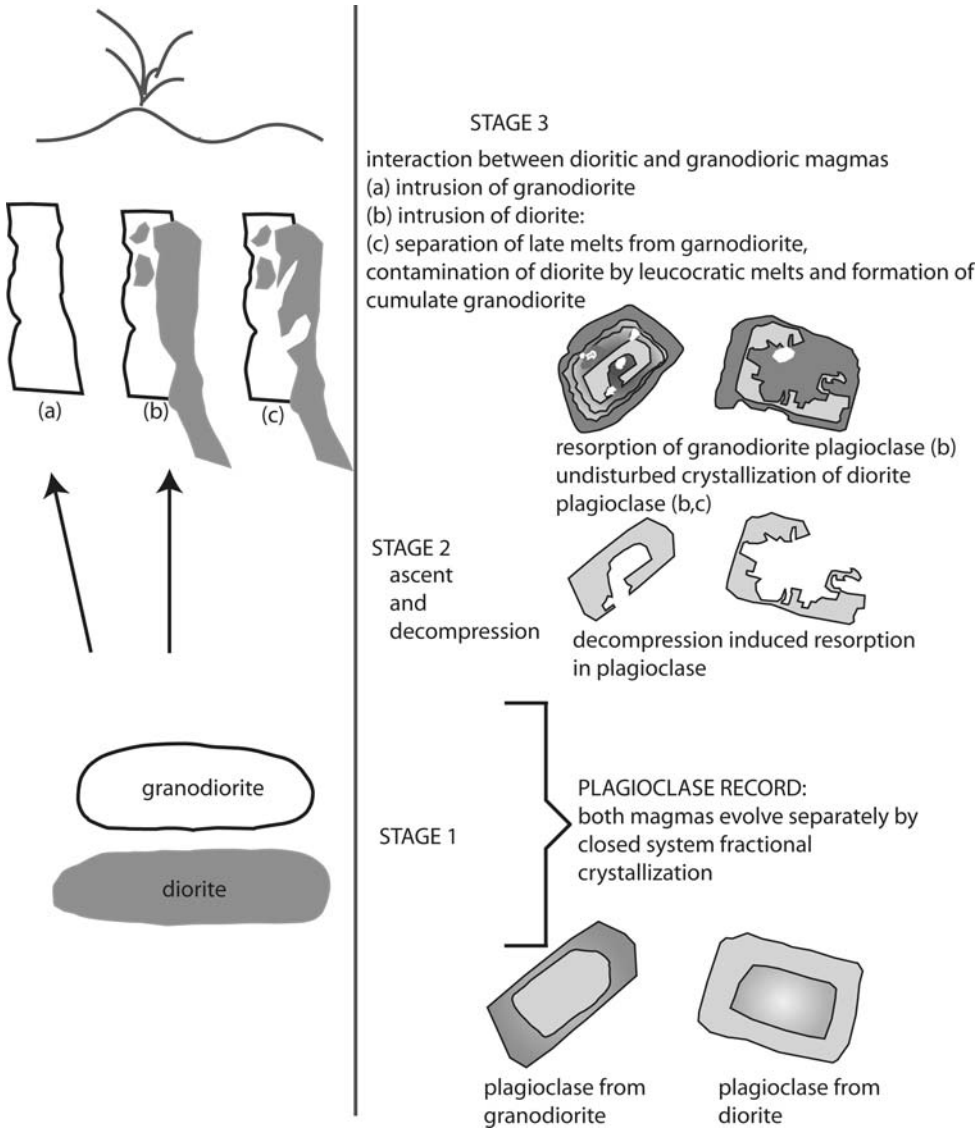

Fig. 13 Model showing evolution of dioritic and granodioritic magmas in the Gęsiniec Intrusion

which took place at lower crustal depths, but without interaction with other magmas (Fig. 13). Such a picture is consistent with magma evolution in small, separate magma chambers that may coalesce and mix upon ascent and emplacement leading to the formation of complex mafic–felsic or felsic–felsic plutons with heterogeneous geochemical and isotopic signatures on scales ranging from individual grains to that of the pluton (e.g., Waight et al. 2000, 2007). Alternatively, magmas parental to the Gesiniec diorites and granodiorites could have undergone hybridization before the onset of plagioclase crystallization (Fig. 13).

The least-contaminated (D30) sample has higher $^{87}Sr/^{86}Sr_{init}$ and lower εNd_{init} (0.7069 and −3.2, respectively, Pietranik and Waight 2008) than those of the bulk earth and depleted mantle at 295 Ma. Similar isotope compositions are observed in other Variscan dioritic-granodioritic associations and they are attributed to contamination of mantle-derived magmas by crustal melts or to derivation from enriched mantle (e.g., Wenzel et al. 1997; Gerdes et al. 2000; Janoušek et al. 2000; Roberts et al. 2000; Janoušek and Holub 2007). Extensive fractional crystallization of mafic, mantle-derived magmas contemporaneous with assimilation of crustal material is supported by the presence of gabbroic cumulates showing a range in Sr ratios and εNd from those close to the depleted mantle to those approaching the values typical of the diorites that form dykes and enclaves in the felsic rocks (e.g., Tribuzio et al. 1999; Sano et al. 2002). If the mafic magmas were hybridized by the crust and vice versa, it would suggest that plagioclase, despite being liquidus phase, records only a limited span of the evolution of the mafic and felsic magmas. In this scenario the evolution of mafic magmas before emplacement would require prolonged fractionation and contamination with more fractioned magmas being effectively separated from cumulus material. An alternative scenario is derivation of dioritic magmas by remelting of old, mafic lower crust (e.g., Zhao et al. 2007; Pietranik and Waight 2008).

Application of plagioclase composition to constrain magma interactions

Whole rock major, trace element, and isotope compositions are routinely used to unravel processes responsible for the interaction of mafic and felsic components in the continental crust. However, it is often difficult unambiguously to constrain which of the many possible processes determined the initial composition of end members. One of the processes that may complicate the geochemical and isotopic picture is the formation of cumulate and late-stage melts that interact with dioritic rocks, as demonstrated here. Major and trace element zonation in some mineral phases can provide robust records of the processes involved, and plagioclase has been shown to record magma differentiation processes such as assimilation or magma mixing at different stages of magma evolution (e.g., Blundy and Shimizu 1991; Singer et al. 1995; Brophy et al. 1996; Hattori and Sato 1996; Tepley et al. 2000; Waight et al. 2000; Ginibre et al. 2002; Halama et al. 2002; Pietranik et al. 2006; Davidson et al. 2007).

We have demonstrated that each plagioclase population develops characteristic features such An_{min} and An versus Or trends that appear to depend on the initial and final compositions of magmas, e.g., K/Na ratio and/or conditions of crystallization (e.g., Hattori and Sato 1996). We argue that An_{min} and An versus Or trends change only when the composition of the melt around the crystallizing plagioclase is drastically changed, as by extensive mixing or convection in the magma chamber and so they remain useful tools to detect such drastic changes. The new results from the Gęsiniec Intrusion presented here appear to support this hypothesis. Cumulate granodiorite clearly represents a system affected by both magma mixing and late stage melt removal, and plagioclase from the granodiorite does not yield common An_{min} for all samples and has scattered An versus Or trends. The conclusions obtained from An_{min} and An versus Or trends are supported by modelling of the An versus Sr in the melt trends. We suggest that to check the robustnes of the methods used here, they should be applied to other mafic–felsic systems, for example, where more extensive mixing is suggested by the transfer of phenocrysts from felsic magma to the enclaves (e.g., Waight et al. 2000; Słaby and Martin 2008), or where mafic injection caused extensive remelting of granite and hybridization of both the mafic and felsic magmas (e.g., Wiebe et al. 2004).The number of grains analyzed from each rock type depends on the complexity of the system being investigated. This study highlights that a small number of grains (∼5) from each rock type provided important constraints on the An_{min} and the An versus Or trends.

Conclusions

The composition and zonation in plagioclase crystals from diorite and granodiorite samples reveal that dioritic magma was not variably hybridized by magma mixing at the level of emplacement, and that the magma mixing process is recorded only in granodioritic magma. In contrast, the compositional variation in the diorites is best explained by subsolidus, or close to solidus, interaction with residual fluids squeezed from the granodioritic crystal mush. This study shows that it is possible to produce a range of whole rock compositions by late stage melt infiltration. The melt can interact with and change composition of mafic phases

such as ambhibole and biotite, but not plagioclase that preserves the composition from the earlier stage of magma evolution.

Simple zonation patterns in plagioclase from both the diorite and the granodiorite suggest that before this late-stage interaction both magmas evolved by closed system fractional crystallization. Any modification of the magmas parental to the granodiorites and the diorites appears to have happened before the onset of the analyzed plagioclase crystallization record. In the case of the diorites this may have involved open system evolution of mafic magmas by assimilation—fractional crystallization with effective separation of evolved melts and cumulus minerals.

Application of An_{min} content in plagioclase and An versus Or and An versus Sr trends for a relatively small number of representative plagioclase grains may provide new insight into mafic–felsic magma interactions. Future work on geochemically and petrologically well defined mingling zones should seek to test this approach.

Acknowledgments The research work was supported by grants to AP: 2022/W/ING/07 and KOLUMB by the Polish Science Foundation. We are grateful to Vojtech Janoušek and Bill Collins for very helpful reviews and editorial comments. Chris Hawkesworth is thanked for valuable comments on an early version of this manuscript, and his suggestions as to how the English might be improved.

Appendix

Calculation of Sr content in melt from Sr plagioclase composition allows for interpreting the change of Sr concentration in plagioclase in terms of contemporaneous change of melt composition. However, despite the obvious appeal of this approach, it requires certain assumptions to be made. They are discussed below:

Recalculation of Sr content in plagioclase to Sr content in the melt from which the plagioclase crystallized assumes equilibrium partitioning between crystal and melt. The equilibrium is not reached if the rate of crystallization is controlled by diffusion of elements to the crystal surface. However, such a kinetic control on crystallization should lead to either oscillatory zoning (e.g., Sibley et al. 1976) or skeletal morphology of plagioclase (Lofgren 1980), none of which is observed in diorites and only some oscillatory zoning occurs in outer parts of granodiorite plagioclase (Pietranik et al. 2006). Also consistent trends in An versus Sr in the melt plot observed for all rocks suggest that the change of Sr concentration in plagioclase is probably reflecting the actual change in melt composition. However, if recalculated Sr content in the melt represents true melt composition, then the value for the first plagioclase to crystallize (probably that with the highest An content) should be close to or higher than the whole rock Sr content since the plagioclase is the only high-temperature phase that concentrates Sr. For that statement to be true requires that the whole rock represents magma composition; however, there is no structural or geochemical reason to expect that the most mafic dioritic rocks are cumulates or hybrid mixtures of minerals derived from different magmas, as will be shown in this paper. The offsets between Sr whole rock content and Sr content in the melt in equilibrium with the cores of plagioclase are $\sim$130 ppm for granodiorite GD15 and $\sim$50–70 ppm for diorite. The offsets are slightly higher than propagated error on Bindeman et al. (1998) equation $RT \ln D_{Sr} = aX_{An} + b$ (1SD = $\sim$30 ppm), where $D_{Sr} = C_{plag}/C_{melt}$ (C_x-concentration of Sr in phase x) assuming individual errors on C_{plag}, T and X_{An} are 90 ppm, 100°C and 1 mol%, respectively. If errors on a and b coefficients are taken into account the propagated error is $\sim$180 ppm, therefore, almost completely overlapping with the range of results for granodiorite and diorite. However, only C_{plag} and X_{An} should contribute to the scatter of the data, whereas changes in T, a and b would increase or decrease calculated C_{melt} of whole set of data. Therefore, we accept that the calculated C_{melt} is only accurate within error $\sim$180 ppm; however precision of the data and thus trends observed in An versus Sr diagram is much better $\sim$30 ppm and can be interpreted as a change of melt composition contemporaneous with plagioclase crystallization.

References

Altherr R, Henes-Klaiber U, Hegner E, Satir M, Langer C (1999) Plutonism in the Variscan Odenwald (Germany): from subduction to collision. Int J Earth Sci 88(3):422–443

Anders E, Grevesse N (1989) Abundances of the elements: meteoritic and solar. Geochim Cosmochim Acta 53(1):197–214

Annen C, Blundy JD, Sparks RSJ (2006) The genesis of intermediate and silicic magmas in deep crustal hot zones. J Petrol 47(3):505–539

Barbarin B (2005) Mafic magmatic enclaves and mafic rocks associated with some granitoids of the central Sierra Nevada batholith, California: nature, origin, and relations with the hosts. Lithos 80(1–4):155–177

Białek J, Pietranik A (2006) Geochemistry and petrology of tonalite and granodiorite from Strzelin crystalline Massif (SW Poland)—comparison. Miner Pol Special Pap 29:103–106

Bindeman IN, Davis AM, Drake MJ (1998) Ion microprobe study of plagioclase-basalt partition experiments at natural concentration levels of trace elements. Geochim Cosmochim Acta 62(7):1175–1193

Blundy JD, Shimizu N (1991) Trace element evidence for plagioclase recycling in calc-alkaline magmas. Earth Planet Sci Lett 102:178–197

Bonin B (2004) Do coeval mafic and felsic magmas in post-collisional to within-plate regimes necessarily imply two contrasting, mantle and crustal, sources? A review. Lithos 78(1–2):1–24

Brophy JG, Dorais MJ, Donnelly-Nolan J, Singer BS (1996) A textural and compositional (ion-probe and electron probe) study of plagioclase zonation styles in hornblende gabbro cumulates from Little Glass Mountain, Medicine Lake volcano, California: implications for fractional crystallization mechanisms in calc-alkaline magma genesis. Contrib Miner Petrol 126:121–136

Collins WJ, Richards SR, Healy BE, Ellison PI (2000) Origin of heterogeneous mafic enclaves by two-stage hybridisation in magma conduits (dykes) below and in granitic magma chambers. Trans R Soc Edinb Earth 91:27–45

Davidson JP, Morgan DJ, Charlier BLA, Harlou R, Hora JM (2007) Microsampling and isotopic analysis of igneous rocks: implications for the study of magmatic systems. Annu Rev Earth Planet Sci 35:273–311

Didier J, Barbarin B (eds) (1991) Enclaves and granite petrology. Amsterdam, Elsevier

Donaire T, Pascual E, Pin C, Duthou JL (2005) Microgranular enclaves as evidence of rapid cooling in granitoid rocks: the case of the Los Pedroches granodiorite, Iberian Massif, Spain. Contrib Miner Petrol 149:247–265

Dorais MJ, Whitney JA, Roden MF (1990) Origin of mafic enclaves in the Dinkey Creek Pluton, Central Sierra-Nevada Batholith, California. J Petrol 31:853–881

Elburg MA (1996) Evidence of isotopic equilibration between microgranitoid enclaves and host granodiorite, Warburton Granodiorite, Lachlan Fold Belt, Australia. Lithos 38(1–2):1–22

Gerdes A, Wörner G, Finger F (2000) Hybrids, magma mixing and enriched mantle melts in post-collisional Variscan granitoids: the Rastenberg Pluton, Austria. In: Franke W, Haak V, Oncken O, Tanner D (eds) Orogenic processes: quantification and modelling in the Variscan Fold Belt, vol 179. Geological Society, London, Special Publication, pp 415–431

Ginibre C, Kronz A, Wörner G (2002) Minor- and trace-element zoning in plagioclase: implications for magma chamber processes at Parinacota volcano, northern Chile. Contrib Miner Petrol 143:300–315

Halama R, Waight T, Markl G (2002) Geochemical and isotopic zoning patterns of plagioclase megacrysts in gabbroic dykes from the Gardar Province, South Greenland: implications for crystallisation processes in anorthositic magmas. Contrib Miner Petrol 144:109–127

Hattori K, Sato H (1996) Magma evolution recorded in plagioclase zoning in 1991 Pinatubo eruption products. Am Mineral 81 (7–8):982–994

Housh T, Luhr JF (1991) Experimental plagioclase-melt equilibria for water-saturated andesite and basalt. Am Mineral 76:477–492

Janoušek V, Holub FV (2007) The causal link between HP-HT metamorphism and ultrapotassic magmatism in collisional orogens: case study from the Moldanubian Zone of the Bohemian Massif. Proc Geol Assoc 118:75–86

Janoušek V, Bowes DR, Rogers G, Farrow CM, Jelinek E (2000) Modelling diverse processes in the petrogenesis of a composite batholith: the Central Bohemian Pluton, Central European Hercynides. J Petrol 41(4):511–543

Janoušek V, Braithwaite CJR, Bowes DR, Gerdes A (2004) Magma-mixing in the genesis of Hercynian calc-alkaline granitoids: an integrated petrographic and geochemical study of the Sazava intrusion, Central Bohemian Pluton, Czech Republic. Lithos 78:67–99

Kemp AIS, Hawkesworth CJ, Foster GL, Paterson BA, Woodhead JD, Hergt JM, Gray CM, Whitehouse MJ (2007) Magmatic and crustal differentiation history of granitic rocks from Hf–O isotopes in zircon. Science 315:980–983

Kocak K (2006) Hybridization of mafic microgranular enclaves: mineral and whole-rock chemistry evidence from the Karamadazi Granitoid, Central Turkey. Int J Earth Sci 95:587–607

Kumar S, Rino V (2006) Mineralogy and geochemistry of microgranular enclaves in Palaeoproterozoic Malanjkhand granitoids, central India: evidence of magma mixing, mingling, and chemical equilibration. Contrib Miner Petrol 152(5):591–609

Lesher CE (1990) Decoupling of chemical and isotopic exchange during magma mixing. Nature 344:235–237

Lofgren GE (1980) Experimental studies on the dynamic crystallization of silicate melts. In: Hargraves RB (ed) Physics of magmatic processes. Princeton University Press, Princeton, pp 487–551

Lorenc M (1984) Enklawy homeogeniczne (autolity) jako wskaźnik magmowego pochodzenia granitoidów strzelińskich. Geol Sudet 19(1):75–97 (in polish)

Nakamura M, Shimakita S (1998) Dissolution origin and syn-entrapment compositional change of melt inclusion in plagioclase. Earth Planet Sci Lett 161:119–133

Oberc-Dziedzic T (1999) The geology of Strzelin Granitoids (Fore-Sudetic Block, SW Poland). Mineral Soc Pol Special Pap 14:22–32

Oberc-Dziedzic T (2002) Polycycle structure of the tonalite-diorite dykes in the Strzelin massif: a result of magmatic differentiation or separated magmatic pulses? Mineral Soc Pol Special Pap 20:159–161

ObercDziedzic T, Pin C, Duthou JL, Couturie JP (1996) Age and origin of Strzelin granitoids (Fore-Sudetic Block, SW Poland): $^{87}Rb/^{86}St$ data. Neues Jb Miner Abh 171:187–198

Oberc-Dziedzic T, Klimas, Kryza R, Fanning CM (2003) SHRIMP U-Pb zircon geochronology of the Strzelin gneiss, SW Poland: evidence for a Neoproterozoic thermal event in the Fore-Sudetic Block, Central European Variscides. Int J Earth Sci 92:701–711

Pietranik A, Waight TE (2008) Processes and Sources during Late Variscan Dioritic-Tonalitic Magmatism: Insights from Plagioclase Chemistry (Gesiniec intrusion, NE Bohemian Massif, Poland). J Petrol 49(9):1619–1645

Pietranik A, Koepke J, Puziewicz J (2006) The study of crystallization and resorption in plutonic plagioclase: implications on evolution of granodiorite magma (Gęsiniec Granodiorite, Strzelin Crystalline Massif, SW Poland). Lithos 86:260–280

Pin C, Binon M, Belin JM, Barbarin B, Clemens JD (1990) Origin of microgranular enclaves in granitoids—equivocal Sr-Nd evidence from Hercynian rocks in the Massif Central (France). J Geophys Res 95:17821–17828

Pitcher WS (1993) The Nature and origin of granite. Blackie Academic and Professional Press, London, pp 117–139

Prouteau G, Scaillet B (2003) Experimental constraints on the origin of the 1991 Pinatubo dacite. J Petrol 44:2203–2241

Roberts MP, Pin C, Clemens JD, Paquette J-L (2000) Petrogenesis of mafic to felsic plutonic rocks associations: the calc-alkaline Quérigut Complex, French Pyrenees. J Petrol 41:809–844

Sano S, Oberhansli R, Romer RL, Vinx R (2002) Petrological, geochemical and isotopic constraints on the origin of the Harzburg intrusion, Germany. J Petrol 43:1529–1549

Sibley DF, Vogel TA, Walker BM, Byerly G (1976) The Origin of Oscillatory Zoning in Plagioclase: A Diffusion and Growth Controlled Model. Am J Sci 276:275–284

Singer BS, Dungan MA, Layne GD (1995) Textures and Sr, Ba, Mg, Fe, K and Ti compositional profiles in volcanic plagioclase: Clues to the dynamics of calc-alkaline magma chambers. Am Mineral 80:776–798

Singh J, Johannes W (1996) Dehydration melting of tonalites. Part II. Composition of melts and solids. Contrib Miner Petrol 125:26–44

Słaby E, Martin H (2008) Mafic and felsic magma interaction in granites: The Hercynian Karkonosze Pluton (Sudetes, Bohemian Massif). J Petrol 49(2):353–391

Słaby E, Götze J, Wörner G, Simon K, Wrzalik R, Śmigielski M (2008) K-feldspar phenocrysts in microgranular magmatic

enclaves: a cathodoluminescence and geochemical study of crystal growth as a marker of magma mingling dynamics. Lithos 105(1–2):85–97

Tepley FJ, Davidson JP, Tilling RI, Arth JG (2000) Magma mixing, recharge and eruption histories recorded in plagioclase phenocrysts from El Chichon Volcano, Mexico. J Petrol 41:1397–1411

Tepper JH, Kuehner SM (2004) Geochemistry of mafic enclaves and host granitoids from the Chilliwack Batholith, Washington: Chemical exchange processes between coexisting mafic and felsic magmas and implications for the interpretation of enclave chemical traits. J Geol 112:349–367

Tribuzio R, Thirlwall MF, Messiga B (1999) Petrology, mineral and isotope geochemistry of the Sondalo gabbroic complex (Central Alps, Northern Italy): implications for the origin of post-Variscan magmatism. Contrib Miner Petrol 136:48–62

Turniak K, Tichomirowa M, Bombach K (2006) Pb-evaporation zircon ages of post-tectonic granitoids from the Strzelin Massif. Min Pol- Special Papers 29:212–215

Tsuchiyama A (1985) Dissolution kinetics of plagioclase in melt of the system diopside-albite-anorthite, and the origin of dusty plagioclase in andesites. Contrib Miner Petrol 89:1–16

Vernon RH, Paterson SR (2008) How late are K-feldspar megacrysts in granites? Lithos 104(1–4):327–336

Waight TE, Maas R, Nicholls IA (2000) Fingerprinting feldspar phenocrysts using crystal isotopic composition stratygraphy: implications for crystal transfer and magma mingling in S-type granites. Contrib Miner Petrol 139:227–239

Waight TE, Maas R, Nicholls IA (2001) Geochemical investigations of microgranitoid enclaves in the S-type Cowra Granodiorite, Lachlan Fold Belt, SE Australia. Lithos 56:165–186

Waight TE, Wiebe RA, Krogstad EJ (2007) Isotopic evidence for multiple contributions to felsic magma chambers: Gouldsboro Granite, Coastal Maine. Lithos 93:234–247

Wenzel T, Mertz DF, Oberhänsli R, Becker T, Renne PR (1997) Age, geodynamic setting, and mantle enrichment processes of a K-rich intrusion from the Meissen massif (northern Bohemian massif) and implications for related occurrences from the mid-European Hercynian. Int J Earth Sci 86:556–570

Wiebe RA (1996) Mafic-silicic layered intrusions: the role of basaltic injections on magmatic processes and the evolution of silicic magma chambers. Trans Roy Soc Edin-Earth 87:233–242

Wiebe RA, Smith D, Sturm M, King EM, Seckler MS (1997) Enclaves in the Cadillac Mountain granite (coastal Maine): samples of hybrid magma from the base of the chamber. J Petrol 38:393–423

Wiebe RA, Manon MR, Hawkins DP, McDonough WF (2004) Late-stage mafic injection and thermal rejuvenation of the Vinalhaven granite, coastal Maine. J Petrol 45:2133–2153

Wright TL, Doherty PC (1977) A linear programming and least squares computer method for solving petrologic mixing problems. Geol Soc Am Bull 81:1995–2008

Zhao ZF, Zheng YF, Wei CS, Wu YB (2007) Post-collisional granitoids from the Dabie orogen in China: Zircon U-Pb age, element and O isotope evidence for recycling of subducted continental crust. Lithos 93:248–272